

# Degradation and Corrosion Behavior of Electrospun PHBV Coated AZ-31 Magnesium Alloy for Biodegradable Implant Applications

J. Castro<sup>1</sup> · K. Gokula Krishnan<sup>1</sup> · S. Jamaludeen<sup>1</sup> · P. Venkataragavan<sup>1</sup> · S. Gnanavel<sup>1</sup>

Received: 20 June 2017 / Revised: 4 October 2017 / Accepted: 5 October 2017 / Published online: 23 October 2017  
© Springer International Publishing AG 2017

**Abstract** The roles of biodegradable materials have been increasing due to its promising and improved features than conventional materials used for biomedical implants. Thus, the need for developing a better biodegradable material is necessary which could deliver better properties for the implants. This present study aims to develop a better biodegradable material where magnesium alloy (AZ-31) chosen as the substrate is surface-modified by annealing followed by a chemical treatment and then PHBV (poly (3-hydroxybutyric acid-co-3-hydrovaleric acid)) having 12% hydroxyvaleric acid content is coated over the modified surface. The coating of the polymer over the sample substrate is done by electrospinning. X-ray diffraction (XRD), field emission scanning electron microscopy (FESEM) and Fourier transform infrared spectroscopy (FTIR) analyses showed successful surface modification and deposition of polymer over the substrate. The degradation behavior of the samples was investigated through immersion studies in simulated body fluid (Hanks' solution). The FESEM images of the coated samples were identified with fibers on the surface even after the immersion for 21 days. The corrosion studies were carried out by potentiodynamic polarization method which proved coated sample has a better corrosion resistance than the bare metal in the SBF solution. Nano-fibrous PHBV coating combined with surface modification seems to be a promising method to tailor the degradation and improve the corrosion resistance of Mg alloys which can be used as a better material for biomedical implants.

**Keywords** Mg alloy (AZ-31) · Electrospinning · Biodegradable implant · PHBV

## 1 Introduction

Magnesium-based alloys have become the new focus for bone implant and cardiovascular implant materials because of their mechanical, electrochemical and biological properties [1–4]. In particular, Mg alloys possess mechanical properties for cardiovascular stents as they have fine microstructural features, high ductility and considerable strength [5]. Nowadays, commercial alloys (AZ series) have been extensively studied as implant materials which are usually alloyed with zinc and aluminum to improve the corrosion resistance where aluminum increases the tensile strength of the alloy [6]. But the metal for implants, especially cardiovascular stent implants, demands slow and homogeneous degradation performance along with high fatigue strength which plays a vital role when the stent is subjected to permanent cyclic load (heart beat) in the blood vessel [7]. However, the key challenge of Mg-based alloys which prevent their use in clinical applications is the rapid corrosion and degradation in the biological environment. Such rapid corrosion causes generation of hydrogen gas which is too fast for the bone/tissue to accommodate, thus degrading its mechanical integrity [8–10]. Therefore, it is essential to overcome these drawbacks of Mg-based alloys before implantation in a physiological environment. Thus, forming a corrosion-resistant surface treatment/coating to prevent the substrate surface to come in direct contact with the environment is one of the corrosion prevention processes for Mg alloys [11, 12]. Surface treatment of substrate involves specific reactions on the surface through

✉ J. Castro  
castro795@gmail.com

<sup>1</sup> Department of Biomedical Engineering, SRM University, Chennai, Tamil Nadu, India

some conversion agents which are more adhesive and corrosion resistive, but for biomedical applications factors like biocompatibility, biodegradability, cell viability and antibiotic ability are easily and better achieved by coating a material (deposited coating) over the substrate surface [13]. Various studies revealed that the degradation has been limited using a polymer/ceramic coating over the surface of Mg alloys [14, 15].

Among various polymers which can be used for coating over a metallic surface, PHBV [poly (3-hydroxybutyric acid-co-3-hydrovaleric acid)] a microbial polyester with biodegradable, non-antigenic, biocompatible properties is seeking more attraction and attention [16]. PHBV is a copolymer of poly (hydroxybutyrate) (PHB) and poly (hydroxyvalerate) (PHV) which are derivatives of PHAs (polyhydroxyalkanoates), a class of biodegradable and biocompatible thermoplastic polyesters produced by various microorganisms (e.g., soil bacteria, blue-green algae and some genetically modified plants), in which they act as an intracellular energy and carbon storage products [17]. The biodegradation of PHB and other PHA derivatives is driven by hydrolysis of the ester bond [18]. Their degradation products, such as a  $\beta$ -hydroxybutyric acid (3HB) and 3-hydroxyvaleric acid, are less acidic than lactic and glycolic acid with pKa values 4.7 [19] and 4.72, respectively. [34]. Mechanisms of PHAs degradation are thermal, enzymatic or hydrolytic. For example, hydrolytic degradation of PHB releases 3HB, which is a normal metabolite in human blood; therefore, in the absence of endotoxin, the biodegradation of PHB produced by bacteria does not cause any physiological reaction. This property provides a unique feature for regeneration and drug delivery applications of PHB and other polymers in the PHA family [20].

Coating of polymer/ceramic substance on the metallic substrate is achieved by various methods such as spin coating, dip coating and vapor deposition techniques. An effective approach that is currently followed for polymer deposition is electrospinning [21, 22] where the fibers are deposited over the metal substrate as fibrous mats. However, only some studies reported the combination of polymer coating over the metal surface using electrospinning. Thus, the aim of this study is to develop a better degradable and corrosion-resistive material by coating a polymeric substance over a metal substrate for biomedical implant applications using electrospinning method to accomplish a better coating procedure, so chemically treated magnesium alloy (AZ-31) is coated with PHBV (poly (3-hydroxybutyric acid-co-3-hydrovaleric acid)) with 12% HV by electrospinning. The characterization of the coated metal was performed followed by degradation and bioactivity analysis.

## 2 Materials and Methods

### 2.1 Sample Preparation

The magnesium alloy sheets AZ-31 (magnesium = 94.8% aluminum = 3% zinc = 1% manganese = 0.2%) were cut into dimensions 10 mm  $\times$  10 mm  $\times$  1 mm, rinsed with acetone and was polished using emery papers with grades up to 2000 in steps. The polished samples were annealed at a temperature of 340 °C which was reported previously [23]. The annealed metal samples were treated with 1 M HNO<sub>3</sub> for 2 min and were cleaned with ethanol for 3 min using ultrasonic bath and dried. The samples were named as AZ-U (uncoated), AZ-AP (as received and polymer coated), AZ-ACP (annealed chemically treated and polymer coated).

### 2.2 Coating Procedure

Polymeric fibers were coated on AZ-AP and AZ-ACP sample surface using electrospinning (Espin Nano unit). The electrospinning of the polymer has resulted in the formation of a fibrous layer on the sample's substrate. The solution for electrospinning was produced by dissolving PHBV polymer of 12% HV (purchased from Sigma-Aldrich) in chloroform/DMF (80/20)% (v/v) at the concentration of PHBV 15% (w/w) by constant stirring at 50 °C for 60 min [24]. The optimum conditions followed at the time of electrospinning were temperature 24 °C, humidity 65%, the collector distance 15 cm and flow rate 2 ml/hr.

### 2.3 Coating Characterizations

The FESEM images of samples were taken using FEI Quanta FEG 200 operated at 10 kv in order to study the coating of the fiber deposition on the sample substrate. The phase compositions of the coated metal were analyzed using X-ray diffraction [PANalytical's X'Pert PRO with Cu K $\alpha$  radiation ( $\lambda$  = 1.542 Å)]. The infrared spectra were obtained using Fourier transform infrared spectroscopy (Agilent Resolutions Pro) in the mid-IR region (400–3000 cm<sup>-1</sup>).

### 2.4 Degradation Studies

The samples AZ-U and AZ-ACP were used in the SBF immersion test. Each sample was placed in a bottle with 10 mL of SBF and kept at the room temperature of (37.5  $\pm$  0.5) °C. Immersion was carried out for 1–21 days. After soaking for the predetermined time, the samples were taken out from the bottle and the pH value of SBF was determined. The surface

morphology and elemental compositions of the samples were also determined.

### 2.5 Electrochemical Measurements

Electrochemical tests were carried out using a Bio-logic VSP potentiostat/frequency response analysis system to evaluate the electrochemical behavior of the samples. Experiments were carried out in a three-electrode electrochemical cell, in which a saturated calomel electrode (SCE) was the reference electrode, a platinum mesh was a counter electrode, and the specimen to be investigated was the working electrode. Potentiodynamic polarization tests were performed at a scan rate of 0.5 mV/s. The polarization curves were used to estimate the corrosion potentials ( $E_{corr}$ ) and corrosion current density ( $i_{corr}$ ) at  $E_{corr}$  by the Tafel extrapolation. The corrosion current is obtained from the Stern–Geary equation where ( $R_p$ ) is the polarization resistance and ( $\beta_a$ ) and ( $\beta_c$ ) are anodic and cathodic Tafel constants, respectively.

$$i_{corr} = \frac{\beta_a \times \beta_c}{2.3 R_p (\beta_a + \beta_c)}$$

## 3 Results and Discussion

### 3.1 FESEM Studies

The FESEM images show the morphology of coated sample with pre-coating treatment (AZ-ACP) (Fig. 1a) where the entire surface of the sample has been evenly distributed with PHBV fibers, whereas the sample which has been directly subjected to coating as received without any treatment (AZ-AP) (Fig. 1b) has sparsely deposited fibers over the surface and uncoated bare metal surface after annealing (Fig. 1c). As observed, the AZ-AP sample showed sparsely distributed fibers, which indicates weak adhesion of the fibers over the substrate surface, and thus in order to increase the adhesive property of the fibrous mats and to form a smooth and uniform coating over the substrate, the AZ-ACP sample is pretreated with  $HNO_3$  which forms a hydroxide layer on the surface, thus increasing the deposition of the polymer uniformly over the substrate [25]. The EDS results have shown the presence of Mg, C, Ca, P, O and Cl. The AZ-ACP samples reported a high percentage of carbon (54.28%) and oxygen (39.23%), which denotes the deposition of polymer over the surface. The presence

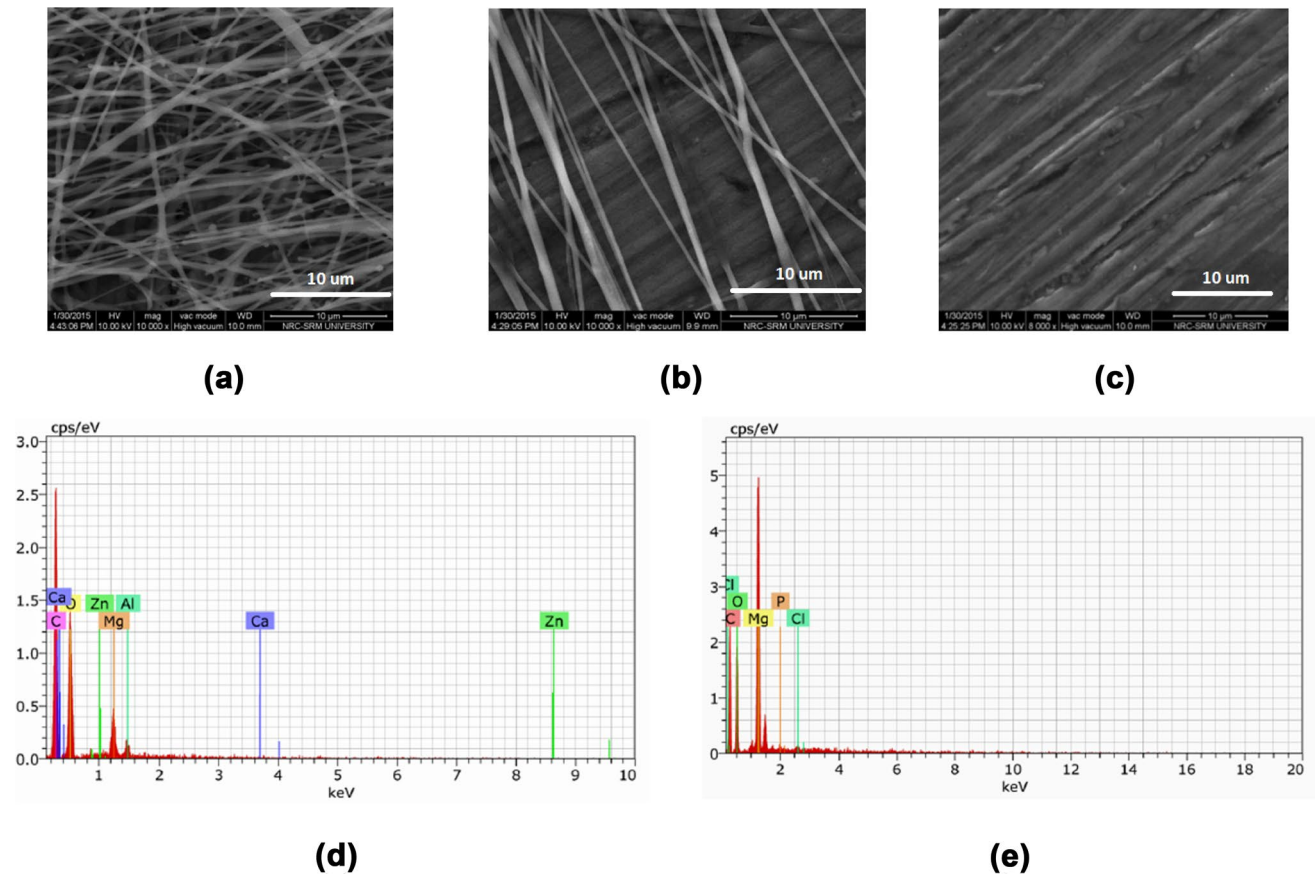


**Fig. 1** FESEM images of samples. AZ-ACP (a), AZ-AP (b), AC-U (c), EDS spectra of AZ-ACP (d) and AZ-AP (e)

of Ca and P is due to HA (hydroxyapatite) and magnesium phosphates formation [26]. The AZ-AP sample showed a decrease in carbon content (16%) with dominating magnesium presence since the surface is not entirely deposited with the polymer [27].

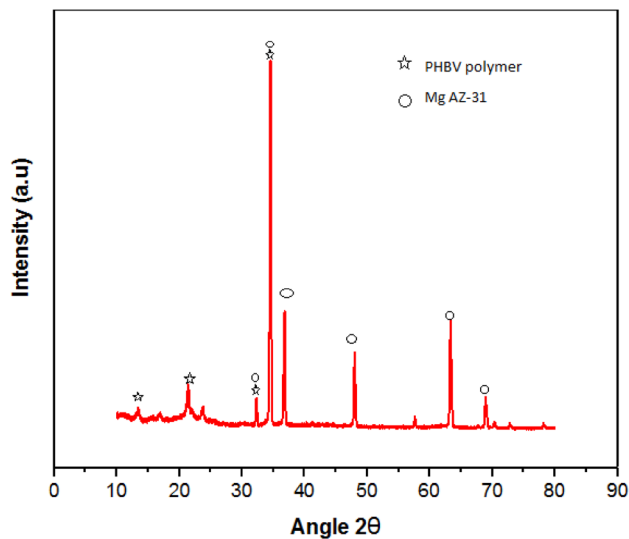


**Fig. 2** X-ray diffraction of PHBV coated Mg AZ-31 sample

### 3.2 X-ray Diffraction Pattern

The XRD patterns of AZ-U and AZ-ACP samples were obtained (Fig. 2). The major peaks of PHBV at  $2\theta$  lie in the region of  $10\text{--}30^\circ$  which was previously reported [28]. The collected spectra of AZ-ACP sample show peaks of PHBV associated with bare Mg AZ-31, particularly between  $30^\circ$  and  $40^\circ$  [29]; which is due to the porous nature of the fibrous mats that the dominating peaks are originating from Mg alloy surface. Moreover, these peaks were enhanced due to the deposition of polymer over the substrate. Thus, the peaks endorse the deposition of a polymeric coating over the surface of the sample.

### 3.3 FTIR Studies

The FTIR spectra performed for AZ-U, PHBV polymer, AZ-ACP samples after coating are shown in Fig. 3a, b, c, respectively. PHBV exhibited a strong band at  $1720\text{ cm}^{-1}$  due to the C=O stretching. Characteristic bands from  $800$  to  $975\text{ cm}^{-1}$  corresponded to symmetric  $\text{--C--O--C--}$  stretching vibration. Moreover, the antisymmetric  $\text{--C--O--C--}$  stretching leads to bands between  $1060$  and  $1150\text{ cm}^{-1}$  [30]. The similar peaks were visible for AZ-ACP sample which signifies the polymer deposition on the AZ-ACP sample surface.

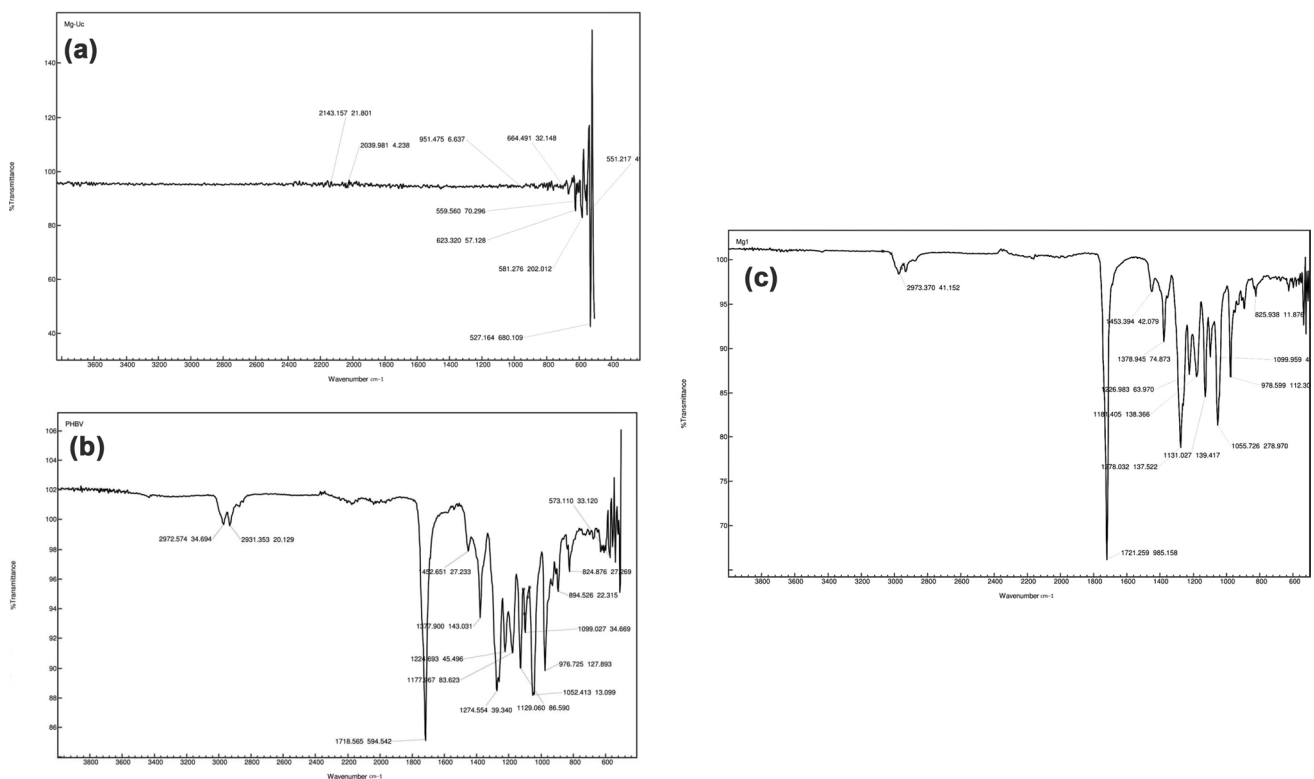


**Fig. 3** FTIR spectra of AZ-U sample (a), PHBV polymer (b), AZ-ACP (c)

### 3.4 In Vitro Characterization

#### 3.4.1 Degradation Morphologies

The photographs of the samples that were subjected to SBF immersion test at 0th day and 21 days are shown in (Fig. 4). The AZ-ACP sample reveals that PHBV coating is sustained which makes the surface to come in less contact with the fluid even after immersion of 21 days, while the AZ-U sample started degrading during the course of immersion.

It is evident from the FESEM images (Fig. 5) showing fibers on the surface of the AZ-ACP sample after 21 days of immersion proving less degradation. The AZ-U sample showed a higher degradation by forming pits and cracks visible on the surface which proves that the coating over the substrate has reduced the degradation rate to that of the uncoated substrate.

Table 1 shows the composition of the elements after the immersion study where AZ-ACP sample has the higher Ca/P ratio which proves better biomineralization [31]. The

high amount of carbon and magnesium present in coated sample proves that the metal is not eroded and degraded while compared to uncoated metal.

#### 3.4.2 pH Value Changes in SBF

Figure 6 shows a lot of variation of pH values as a function of the immersion time. Both samples showed an increase in pH value after 21 days. However, the pH values of solution corresponding to AZ-ACP sample showed a minor pH value change than to AZ-U sample. This change in pH is due to the corrosion of Mg and its alloys [32], and it can be concluded that coated alloys are more corrosion resistive than uncoated alloys. Furthermore, it has been previously reported that a physiological condition with high pH values does not promote cell growth [33] since large pH variations are a hindrance in using Mg alloys as suitable implant materials; this PHBV coated alloy (AZ-ACP) can tailor this requirement with more corrosion resistance.



**Fig. 4** Photographs of AZ-ACP before immersion (a), after immersion (b), AZ-U sample before immersion (c), after immersion (d)

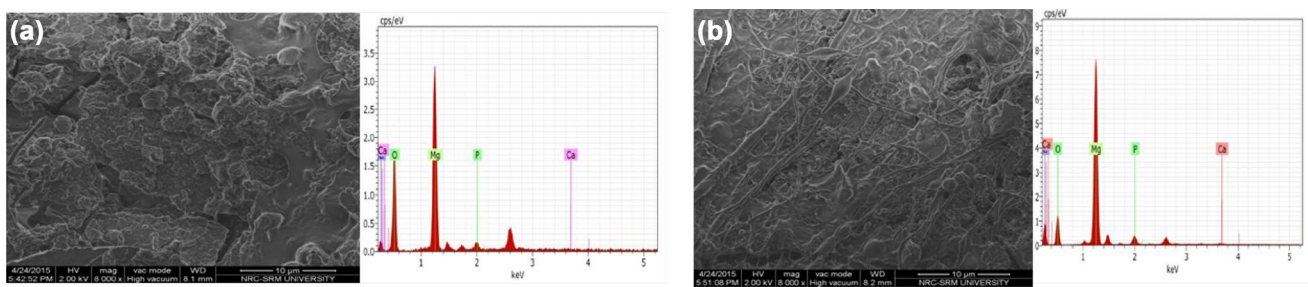


**Fig. 5** FESEM and EDS analysis of AZ-U (a) and AZ-ACP samples (b) after 21 days of immersion study

**Table 1** Elemental composition of the surfaces after 21 days of immersion

Sample	Mg wt%	O wt%	Ca wt%	P wt%	C wt%	Ca/P ratio
AZ-U	13.37	26.26	0.03	0.67	7.74	0.04
AZ-ACP	27.61	32.33	0.15	1.20	36.35	0.12

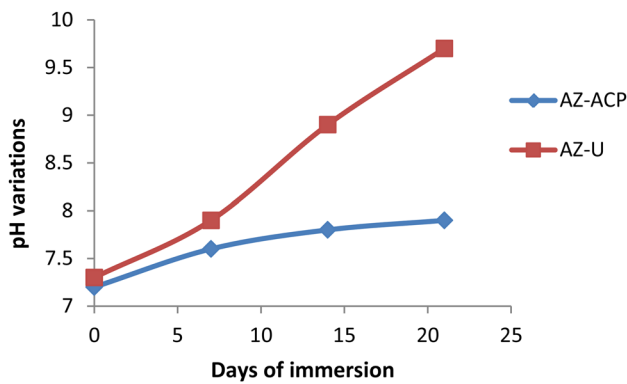


**Fig. 6** pH variations of the samples during the immersion tests in SBF

### 3.5 Electrochemical Characterization

Potentiodynamic polarization curves obtained from AZ-U and AZ-ACP sample substrates in SBF are displayed in (Fig. 7). It could be seen that the corrosion potential ( $E_{\text{corr}}$ ) of AZ-U sample substrate  $-1.396$  V is more negative, while the AZ-ACP sample shows a nobler shift to the  $E_{\text{corr}}$  value  $-1.210$  V. The positive potential shift and decrease in current density show that the corrosion resistance of AZ-ACP sample improved significantly. Moreover, the polarization resistance of the AZ-ACP sample is comparatively higher than that of AZ-U sample, which denotes high corrosion resistance in the environmental fluid.

The electrochemical parameters of potentiodynamic polarization curves are given in Table 2. It can be determined that the PHBV deposition over the surface could control the diffusion of electrolyte into the substrate and thereby

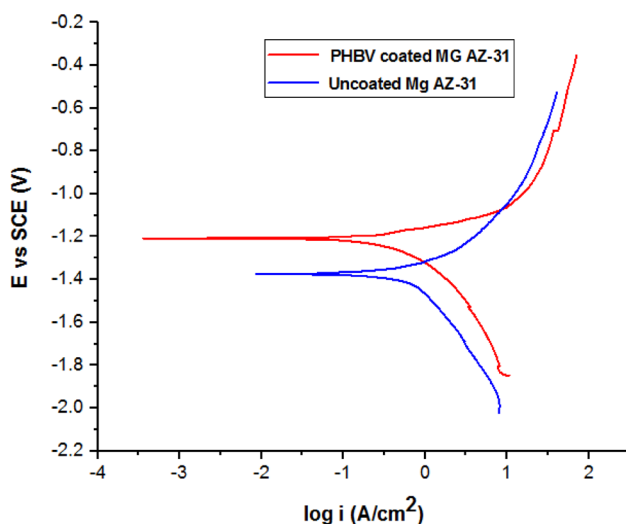


**Fig. 7** Potentiodynamic plots of uncoated and PHBV coated Mg AZ-31 sample

**Table 2** Corrosion potential ( $E_{\text{corr}}$ ) and current density ( $i_{\text{corr}}$ ) values of the samples

Sample	$E_{\text{corr}}$ V	$I_{\text{corr}}$ $\mu\text{A}/\text{cm}^2$	$R_p$ $\Omega \text{ cm}^2$
AZ-ACP	-1.210	78.0	54,069.12
AZ-U	-1.396	163.2	19,968.67

decrease the degradation rate and enhance the potential of AZ-ACP sample than that of the AZ-U sample.

## 4 Conclusion

Electrospun biodegradable PHBV fibers combined with surface modification on Mg AZ-31 alloy served to provide a protective coating over the surface of the substrate. The FESEM images of the AZ-ACP sample denote uniform deposition of the polymer where the metal contact with the physiological medium is reduced which prolongs the degradation, whereas the AZ-AP sample has minimum coverage, so it degrades faster. The SBF immersion studies were carried out for short duration which can be increased to study the long-term effects of the coating over the surface. Though the stoichiometric ratio of Ca/P is lower for the AZ-ACP samples when compared with that of the standard value 1.67, it is higher than the AZ-U sample; hence, it can be further improved by optimizing the coating parameters to obtain better biomineralization. To conclude, this preliminary study can be expanded in further researches which include cell studies and in vivo characterizations for the development of better biodegradable materials for biomedical implant applications, with improved corrosion and degradation rate.

**Acknowledgements** The authors thank and acknowledge Nanotechnology Research Centre and Department of Chemistry, SRM University, India, for their support in the laboratory, characterization and corrosion studies.

### Compliance with Ethical Standards

**Conflict of interest** On behalf of all the authors, the corresponding author states that there is no conflict of interest.

## References

- Zheng YF, Gu XN, Witte F (2014) Biodegradable metals. *Mater Sci Eng R Rep* 77:1–34
- Virtanen S (2011) Biodegradable Mg and Mg alloys: corrosion and biocompatibility. *Mater Sci Eng B* 176(20):1600–1608
- Mueller WD, Lucia Nascimento M, Lorenzo de Mele MF (2010) Critical discussion of the results from different corrosion studies of Mg and Mg alloys for biomaterial applications. *Acta Biomater* 6(5):1749–1755

4. Zhang Y et al (2010) Characterization and degradation comparison of DLC film on different magnesium alloys. *Surf Coat Technol* 205(Supplement 1):S15–S20
5. Witte F et al (2008) Degradable biomaterials based on magnesium corrosion. *Curr Opin Solid State Mater Sci* 12(5–6):63–72
6. Mochizuki A, Kaneda H (2015) Study on the blood compatibility and biodegradation properties of magnesium alloys. *Mater Sci Eng C* 47:204–210
7. Hanzi AC et al (2010) On the in vitro and in vivo degradation performance and biological response of new biodegradable Mg-Y-Zn alloys. *Acta Biomater* 6(5):1824–1833
8. da Conceição TF et al (2012) Controlled degradation of a magnesium alloy in simulated body fluid using hydrofluoric acid treatment followed by polyacrylonitrile coating. *Corros Sci* 62:83–89
9. Alvarez-Lopez M et al (2010) Corrosion behaviour of AZ31 magnesium alloy with different grain sizes in simulated biological fluids. *Acta Biomater* 6(5):1763–1771
10. Uddin MS, Colin H, Peter M (2015) Surface treatments for controlling corrosion rate of biodegradable Mg and Mg-based alloy implants. *Sci Technol Adv Mater* 16(5):053501
11. Song S et al (2012) Corrosion study of new surface treatment/coating for AZ31B magnesium alloy. *Surf Eng* 28(7):486–490
12. Sasikumar Y et al (2017) Effect of surface treatment on the bioactivity and electrochemical behavior of magnesium alloys in simulated body fluid. *Mater Corros* 68:776–790. doi:10.1002/maco.201609317
13. Hornberger H, Virtanen S, Boccaccini AR (2012) Biomedical coatings on magnesium alloys—A review. *Acta Biomater* 8(7):2442–2455
14. Yuan T et al (2016) Fabrication of a delaying biodegradable magnesium alloy-based esophageal stent via coating elastic polymer. *Materials* 9(5):384
15. Tian P, Liu X, Ding C (2015) In vitro degradation behavior and cytocompatibility of biodegradable AZ31 alloy with PEO/HT composite coating. *Coll Surf B Biointerfaces* 128:44–54
16. Lu LX et al (2012) The effects of PHBV electrospun fibers with different diameters and orientations on growth behavior of bone-marrow-derived mesenchymal stem cells. *Biomed Mater* 7(1):015002
17. Li X et al (2009) Improving hydrophilicity, mechanical properties and biocompatibility of poly[(R)-3-hydroxybutyrate-co-(R)-3-hydroxyvalerate] through blending with poly[(R)-3-hydroxybutyrate]-alt-poly(ethylene oxide). *Acta Biomater* 5(6):2002–2012
18. Boskhomdzhiev AP et al (2010) Biodegradation kinetics of poly(3-hydroxybutyrate)-based biopolymer systems. *Biochemistry (Moscow) supplement series B: biomedical. Chemistry* 4(2):177–183
19. Dahl SR, Olsen KM, Strand DH (2012) Determination of gamma-hydroxybutyrate (GHB), beta-hydroxybutyrate (BHB), pregabalin, 1,4-butane-diol (1,4BD) and gamma-butyrolactone (GBL) in whole blood and urine samples by UPLC-MSMS. *J Chromatogr B Anal Technol Biomed Life Sci* 885–886:37–42
20. Manavitehrani I et al (2016) Biomedical applications of biodegradable polyesters. *Polymers* 8(1):20
21. Tong H-W, Wang M (2008) Electrospinning of fibrous PHBV tissue engineering scaffolds: fiber diameter control, fiber alignment and mechanical properties. The 5th International Conference on Information Technology and Application in Biomedicine (ITAB 2008), in conjunction with the 2nd International Symposium & Summer School on Biomedical and Health Engineering, Shenzhen, China, 30–31 May 2008. In: *Proceedings of the ITAB*, pp 535–538
22. Xie J, Li X, Xia Y (2008) Putting electrospun nanofibers to work for biomedical research. *Macromol Rapid Commun* 29(22):1775–1792
23. Soujanya GK et al (2014) Electrospun nanofibrous polymer coated Magnesium alloy for biodegradable implant applications. *Proc Mater Sci* 5:817–823
24. Wagner A et al (2014) Analysis of porous electrospun fibers from Poly(l-lactic acid)/Poly(3-hydroxybutyrate-co-3-hydroxyvalerate) blends. *ACS Sustain Chem Eng* 2(8):1976–1982
25. Hatami M, Saremi M, Naderi R (2015) Improvement in the protective performance and adhesion of polypyrrole coating on AZ31 Mg alloys. *Prog Nat Sci Mater Int* 25(5):478–485
26. Wang Y et al (2008) Corrosion process of pure magnesium in simulated body fluid. *Mater Lett* 62(14):2181–2184
27. Tian P, Liu X (2015) Surface modification of biodegradable magnesium and its alloys for biomedical applications. *Regen Biomater* 2(2):135–151
28. Yu H, Yan C, Yao J (2014) Fully biodegradable food packaging materials based on functionalized cellulose nanocrystals/poly(3-hydroxybutyrate-co-3-hydroxyvalerate) nanocomposites. *RSC Adv* 4(104):59792–59802
29. Amaravathy P et al (2012) Evaluation of in vitro bioactivity and MG63 osteoblast cell response for TiO<sub>2</sub> coated magnesium alloys. *J Sol-Gel Sci Technol* 64(3):694–703
30. Farago PV et al (2008) Physicochemical characterization of a hydrophilic model drug-loaded PHBV microparticles obtained by the double emulsion/solvent evaporation technique. *J Braz Chem Soc* 19:1298–1305
31. Hanas T et al (2016) Tailoring degradation of AZ31 alloy by surface pre-treatment and electrospun PCL fibrous coating. *Mater Sci Eng C Mater Biol Appl* 65:43–50
32. Chunxi Y et al (2010) Effects of magnesium alloys extracts on adult human bone marrow-derived stromal cell viability and osteogenic differentiation. *Biomed Mater* 5(4):045005
33. Geng F et al (2009) The preparation, cytocompatibility, and in vitro biodegradation study of pure  $\beta$ -TCP on magnesium. *J Mater Sci Mater Med* 20(5):1149–1157
34. Volova TG (2004) Polyhydroxyalkanoates—Plastic materials of the 21st century: production, properties, applications. Nova Science Publishers, New York